

## Modeling of the human pilot time delay using Padé series

RÓBERT SZABOLCSI

*Miklós Zrínyi National Defence University, Budapest, Hungary*

*Investigation of the human behavior is in the focus of attention of researchers since many decades. This problem is actual and important also present day. Main purpose of the author is to summarize theoretical backgrounds dealing with mathematical modeling of the human pilot behavior. Second interesting topic being investigated is to give some approximated models of the human pilot applying Padé approximation method. Importance of this paper is in derivation and application of higher order Padé approximants to model human pilot behavior. This new approach allows to model pilot behavior more precisely than before with applying the common first order approximants. The lower and higher order approximants will be analyzed both in time and in frequency domain. A new MATLAB embedded m-file is created by the author to analyze pilot mathematical models.*

### 1. Introduction

Early pioneers of mathematical modeling of the pilots' behavior were McRuer and Krendel.<sup>1</sup> Scientific results of their glorious artwork affect research work of many scientists involved into mathematical modeling of human behavior since many years. This report deals with mathematical modeling of human pilots, with analysis of the pilot's behavior both in single input-single output and multi input-multi output automatic flight control systems. Regarding<sup>1</sup> mathematical model of the human pilots depends also on the feature of signals to be followed by the pilot. Authors are emphasizing importance of problems of precise navigation tasks such as offensive and defensive air-to-air combat, air to ground weapon delivery, formation flight etc. Authors introduced term of *paper pilot*, which means mathematical model of the pilot as 'element' of the automatic flight control system and widely applied in automatic flight control systems' analysis and preliminary design.<sup>1</sup>

In this paper mathematical handbook of Korn and Korn is cited as main source for mathematical backgrounds of the problems of approximating time delay.<sup>2</sup>

Textbooks of Aslanyan<sup>3</sup> and, Krasovsky et al.<sup>4</sup> deal with many aspects of the automatic flight control systems. One of the problems outlined in<sup>3,4</sup> is summary of the mathematical models applied for deriving human pilot behavior. In these books the so-

---

Received: June 7, 2007

*Address for correspondence:*

RÓBERT SZABOLCSI

Miklós Zrínyi National Defence University

P. O. Box 15, H-1581 Budapest, Hungary

E-mail: szabolcsi.robort@zmne.hu

called *pilot-in-the-loop* analysis problem is discussed in detail using Bode method based on classical control theory.

McLean<sup>5</sup> in deals with conventional and modern mathematical modeling of the human pilot behavior making difference between aircraft and helicopter pilots. In Reference 5 time delay of human pilot is approximated by first order Padé approximation, which may be unsatisfactory and time delay may be approximated by higher order approximants of Padé-series.<sup>5</sup>

Dorf and Bishop derived mathematical model of human operator, which has more extended applicability. In this mean, human operator models can be applied for any kind of drivers (e.g.m car, motorcycle, ship, train, aircraft etc.). Obviously, the only common thing these models are coinciding is the feature of the mathematical models, while their parameters are different.<sup>6</sup>

Finally, author of this paper leans on his preliminary scientific papers dealing with conventional and modern mathematical methods applied for modeling human pilot behavior,<sup>8</sup> derivation critical parameters of the human pilot acting in the closed loop flight control system,<sup>9</sup> and, derivation of the complex set of critical parameters of the human pilot in the aircraft lateral motion flight control systems.<sup>10</sup>

Computer aided simulation was executed by using MATLAB computer package supplemented with Control System Toolbox.<sup>11,12,13</sup>

## 2. Padé approximation of the time delay

Let us consider dynamical system given in Figure 1. Transfer function of  $G(s)$  represents dynamical system consisting of time delay of  $\tau$ , and transfer function of  $G_0(s)$ , which is supposed to be strictly proper and stable. The problem of approximation of the time delay can be formulated as follows: approximate original transfer function of

$$G(s) = e^{-s\tau} G_0(s) \quad (2.1)$$

by an approximated transfer function of

$$\hat{G}(s) = P_d(s)G_0(s), \quad (2.2)$$

where  $P_d(s) = N_d(s)/D_d(s)$  is a rational approximation of time delay of  $\tau$ . In other words, we want to find transfer function of  $P_d(s)$  so that closed loop behavior of  $\hat{G}(s)$  matches input-output behavior of the original system represented by  $G(s)$ .

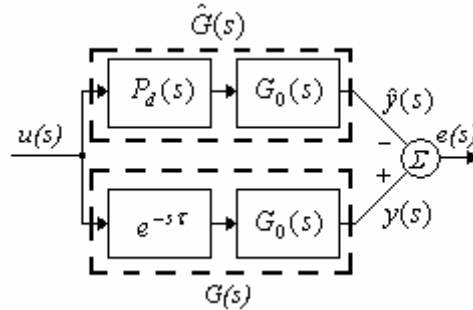


Figure 1. The model matching error problem

To measure the error of approximation  $e(s)$  we will apply the same input  $u(s)$  to both of transfer functions of  $G(s)$ , and  $\hat{G}(s)$ , respectively. By comparing output signals of  $y(s)$  and  $\hat{y}(s)$  one can derive how  $\hat{G}(s)$  approximates  $G(s)$ . In other words, how  $P_d(s)$  approximates time delay defined by  $e^{-s\tau}$ . In control theory this problem is formulated as the so-called *model matching problem*.<sup>2,7</sup> The model-matching error (MME) can be derived using following equation:

$$MME \triangleq \sup_{u \neq 0} \frac{\|e\|_2}{\|u\|_2} = \sup_{u \neq 0} \frac{\|y - \hat{y}\|_2}{\|u\|_2} \quad (2.3)$$

In equation (2.3)  $\|y - \hat{y}\|_2$  denotes quadratic (Euclidean) norm of output error vector of  $e = y - \hat{y}$  due to quadratic (Euclidean) norm of input signal of  $\|u\|_2$ . The largest possible ratio of output error energy over input energy is defined as model-matching error. It is well-known from control theory that model-matching error can be defined as:

$$MME \equiv MME_{H_\infty} \equiv MME_{L_\infty}, \quad (2.4)$$

where

$$MME_{H_\infty} = \|G - \hat{G}\|_{H_\infty}, \quad (2.5)$$

$$MME_{L_\infty} = \sup_{\omega} |G(j\omega) - \hat{G}(j\omega)| = \sup_{\omega} |G_0(j\omega)| \cdot \left| e^{-j\omega\tau} - P_d(j\omega) \right|. \quad (2.6)$$

It is obvious, that if  $MME_{L_\infty}$  is small, than difference between the Nyquist plots of transfer functions of  $G(s)$  and  $\hat{G}(s)$  is small. This observation is valid if and only if

$G_0(s)$  is strictly proper and stable. Therefore, for given transfer function of  $G_0(s)$  we want to find a rational approximation of  $P_d(s)$  for the pure time delay derived by  $e^{-s\tau}$  so that approximation error, i.e. model-matching error  $MME_{L_\infty}$  is smaller than a pre-defined positive tolerance, say  $\delta > 0$ .

For further discussion of Padé approximation there will used following formula:<sup>7,8,9,10</sup>

$$e^{-s\tau} \cong P_d(s) = \frac{N_d(s)}{D_d(s)} = \frac{\sum_{k=0}^n (-1)^k c_k \tau^k s^k}{\sum_{k=0}^n c_k \tau^k s^k}, \quad (2.7)$$

where coefficients of equation (2.7) are defined as follows:

$$c_k = \frac{(2n-k)! \cdot n!}{2n! \cdot k! \cdot (n-k)!}; \quad n = 1, 2, 3, 4, \dots; \quad k = 0, 1, 2, 3, \dots, n. \quad (2.8)$$

### 2.1. Model order selection for Padé approximation

During solution of problems of control system's analysis and design a simple question may arise: what is the minimum order of the Padé approximation, which results in maximum permissible approximation error? Section 2.1 is about of answering this problem, and deals with this problem giving recommendations for its solution. The approximation error easily can be found from equation (2.6) as given below:

$$\left| e^{-j\omega\tau} - P_d(j\omega) \right| \leq \begin{cases} 2 \left( \frac{e\omega\tau}{4n} \right)^{2n+1}, & \text{if } \omega \leq \frac{4n}{e\tau} \\ 2, & \text{if } \omega \geq \frac{4n}{e\tau} \end{cases}. \quad (2.9)$$

Using equation (2.9) the so-called *model order selection problem* can be solved via following steps to be strictly followed:

**Step 1.** Using magnitude plot of  $G_0(j\omega)$  find the frequency of  $\omega_x$  such that

$$\left| G_0(j\omega) \right| \leq \frac{\delta}{2} \text{ for all } \omega \geq \omega_x, \quad (2.10)$$

and for the first step, let us initialize  $n = 1$ .

**Step 2.** For each set of  $n \geq 1$  define

$$\omega_n = \max \left\{ \omega_x, \frac{4n}{e\tau} \right\}, \quad (2.11)$$

and plot the error magnitude function using following formula:

$$\varepsilon(\omega) \doteq \begin{cases} 2|G_0(j\omega)| \left( \frac{e\omega\tau}{4n} \right)^{2n+1}, & \text{for } \omega \leq \frac{4n}{e\tau} \\ 2|G_0(j\omega)|, & \text{for } \omega_n \geq \omega \geq \frac{4n}{e\tau} \end{cases}. \quad (2.12)$$

**Step 3.** Let us define

$$E(n) = \frac{1}{\delta} \max \{ \varepsilon(\omega) \}; \quad \omega \in [0, \omega_x]. \quad (2.13)$$

If  $E(n) \leq 1$ , then stop. In this case value of  $n$  satisfies the desired error bound, in other words:

$$MME_{L_\infty} \leq \delta. \quad (2.14)$$

Otherwise, increase  $n$  by 1, and go to Step 2.

**Step 4.** Plot the approximation error function of

$$|G_0(j\omega)| \cdot \left| e^{-j\omega\tau} - P_d(j\omega) \right| \quad (2.15)$$

versus frequency, and verify graphically that its peak value is less than  $\delta$ .

Since transfer function  $G_0(s)$  is strictly proper algorithm given above will pass Step 3 eventually for some finite  $n \geq 1$ . At each step of iteration we must draw the error function of  $\varepsilon(\omega)$  defined by equation (2.12) and check whether its peak is less than pre-defined scalar of  $\delta$ . For high precision calculus it is regarded to take into consideration tolerance of  $\delta = (10^{-4} - 10^{-2})$ . On the contrary, it is well-known from theory of automatic control systems that, for instance, settling time is defined for envelope of  $\pm 2\%$ , or of  $\pm 5\%$  due to steady-state value of step response function denoted by  $x_{ss}(\infty)$ . From these thoughts it is evident that mathematical requirements and requirements coming from control theory may conflict and accuracy may be defined making some compromise, which is common and widely used during solution of control system design problems.

### 3. Mathematical models of the human pilot

This section basically follows<sup>1,3,4,5</sup> and preliminary research papers of the author.<sup>8,9,10</sup> The simplest mathematical model of human operator – supposing single reference signal tracking – can be derived using Figure 2:<sup>3,4,5</sup>

$$Y_p(s) = \frac{x_{out}(s)}{x_{in}(s)} = K_p e^{-s\tau}, \quad (3.1)$$

where  $x_{in}$  is the signal to be tracked by the operator,  $x_{out}$  is the response signal of the pilot,  $K_p$  is the pilot gain, and finally,  $\tau$  is the pure time delay.

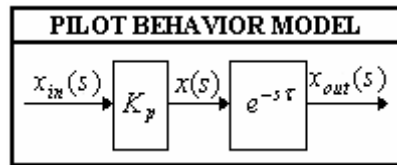


Figure 2. Mathematical model of the pilot behavior

From equation (3.1) it is easily can be seen that the human operator behaves as a proportional (P) controller with time delay (TD).<sup>8,9,10</sup> For more simplicity let us denote equation (3.1) as *P-TD*-model.

More complicated mathematical model of human operator including ability of the pilot to predict any kind of events can be derived using Figure 3:<sup>1,3,4,5</sup>

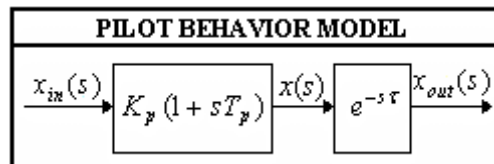


Figure 3. Mathematical model of the human pilot behavior

$$Y_p(s) = \frac{x_{out}(s)}{x_{in}(s)} = K_p (1 + sT_p) e^{-s\tau}, \quad (3.2)$$

where  $T_p$  is prediction time constant. From equation (3.2) it is easily can be derived that the human operator behaves as a proportional-differential (PD) controller with pure time delay (TD).<sup>8,9</sup> For simplicity and further discussion let us denote mathematical model of equation (3.2) as *PD-TD*-model.

Next let us take into consideration dynamic model of the muscular acting system of the human operator. Block diagram of the human operator for this particular case can be seen in Figure 4.

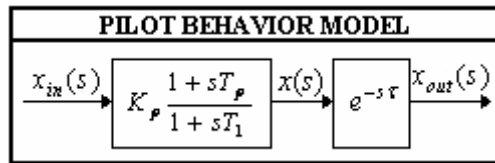


Figure 4. Mathematical model of the pilot behavior

Using Figure 4 transfer function of the pilot can be derived as it given below:

$$Y_p(s) = \frac{x_{out}(s)}{x_{in}(s)} = K_p \frac{1 + sT_p}{1 + sT_1} e^{-s\tau}, \tag{3.3}$$

where  $T_1$  is time constant of the pilot muscular system. From equation (3.3) it easily can be derived that mathematical model of the human operator is proportional-differential (PD) first order (IO) controller having pure time delay (TD).<sup>5,6,8,9,10</sup> For further discussions let us denote equation (3.3) as *PD-IO-TD-model*. Using Figure 4, the following equation can be derived:

$$Y_p(s) = \frac{x_{out}(s)}{x_{in}(s)} = \frac{x(s)}{x_{in}(s)} \frac{x_{out}(s)}{x(s)} = K_p \frac{1 + sT_p}{1 + sT_1} e^{-s\tau}. \tag{3.4}$$

Doing some simple arrangements in equation (3.4) one can write that:

$$x(s) = K_p \frac{1 + sT_p}{1 + sT_1} x_{in}(s). \tag{3.5}$$

Input signal  $x(t)$  of the time delay term of  $\tau$  can be found using following formula:

$$\dot{x} = -\frac{1}{x} + \frac{K_p}{T_1} x_{in} + \frac{K_p T_p}{T_1} \dot{x}_{in}. \tag{3.6}$$

For approximation of time delay of  $\tau$ , in equation (3.3)–(3.5) we will use 1st order Padé approximants. One can write that

$$Y_p(s) = \frac{x_{out}(s)}{x_{in}(s)} = K_p \frac{1 + sT_p}{1 + sT_1} e^{-s\tau} = K_p \frac{1 + sT_p}{1 + sT_1} \left( -\frac{s - 2/\tau}{s + 2/\tau} \right). \tag{3.7}$$

Modern mathematical representation of human operator can be given using its state space representation.<sup>5,6,7,8</sup> During derivation of this dynamical model let us choose state variables as they are given below:

$$x_1 = x_{out} + x, \tag{3.8}$$

$$x_2 = x. \tag{3.9}$$

Using equations (3.3)–(3.9) state and output equations of human pilot – defined on Figure 4 – can be found as follows:<sup>1,8,9,10</sup>

$$\begin{bmatrix} \dot{x}_1 \\ \dot{x}_2 \end{bmatrix} + \begin{bmatrix} 0 \\ -\frac{K_p T_p}{T_1} \end{bmatrix} x_{in} = \begin{bmatrix} -\frac{2}{\tau} & \frac{4}{\tau} \\ 0 & -\frac{1}{T_1} \end{bmatrix} \begin{bmatrix} x_1 \\ x_2 \end{bmatrix} + \begin{bmatrix} 0 \\ \frac{K_p}{T_p} \end{bmatrix} x_{in}, \tag{3.10}$$

$$x_{out} = [1 \quad -1] \begin{bmatrix} x_1 \\ x_2 \end{bmatrix}. \tag{3.11}$$

Finally, by considering the neuro-muscular sensing, processing and, actuating system of the human operator, the block diagram of Figure 5 can be given:<sup>1,8,9,10</sup>

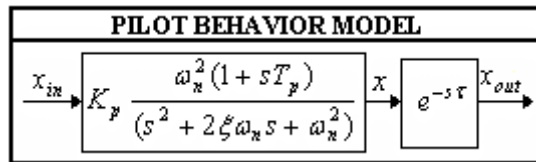


Figure 5. Mathematical model of the human pilot behavior

Using Figure 5, the following transfer function of human pilot can be derived:<sup>1,9,10</sup>

$$Y_p(s) = \frac{x_{out}(s)}{x_{in}(s)} = \frac{x_{out}(s)}{x(s)} \frac{x(s)}{x_{in}(s)} = K_p \frac{\omega_n^2(1+sT_p)}{(s^2 + 2\xi\omega_n s + \omega_n^2)} e^{-s\tau}. \tag{3.12}$$

In equation (3.12) the second order term of

$$\frac{\omega_n^2}{(s^2 + 2\xi\omega_n s + \omega_n^2)} \tag{3.13}$$

defines the simplified mathematical model of the neuro-muscular system of human pilot.<sup>1</sup> It is easy to derive that the second order proportional-differential term of equation (3.12)



$$Y = \frac{x(s)}{x_{in}(s)} = K_p \frac{\omega_n^2(1 + sT_p)}{(s^2 + 2\xi\omega_n s + \omega_n^2)} \quad (3.14)$$

may be rewritten in the following state space model:

$$\begin{bmatrix} \dot{x}_1 \\ \dot{x}_2 \end{bmatrix} = \begin{bmatrix} 0 & 1 \\ -\omega_n^2 & -2\xi\omega_n \end{bmatrix} \begin{bmatrix} x_1 \\ x_2 \end{bmatrix} + \begin{bmatrix} 0 \\ 1 \end{bmatrix} x_{in}, \quad (3.15)$$

$$x = \omega_n^2 K_p \begin{bmatrix} 1 & T_p \end{bmatrix} \begin{bmatrix} x_1 \\ x_2 \end{bmatrix}. \quad (3.16)$$

From equation (3.12) it is easily can be derived that mathematical model of the human pilot is proportional-differential (PD) second order (2O) term having pure time delay (TD).<sup>1,8,9,10</sup> For further discussions let us denote equation (3.12) as *PD-2O-TD*-model.

Let us introduce following state variable

$$x_3 = x_{out} + x. \quad (3.17)$$

Pure time delay of  $\tau$  in equation (3.12) can be approximated using first order Padé approximants. Now one can write that

$$e^{-s\tau} = -\frac{s - 2/\tau}{s + 2/\tau}. \quad (3.18)$$

Let us substitute equation (3.18) into equation (3.12), and convert this mathematical model into time domain one. After several mathematical manipulations one can get following state and output equations:<sup>1,8,9,10</sup>

$$x = \begin{bmatrix} \dot{x}_1 \\ \dot{x}_2 \\ \dot{x}_3 \end{bmatrix} = \begin{bmatrix} 0 & 1 & 0 \\ -\omega_n^2 & -2\xi\omega_n & 0 \\ \left(\frac{4}{\tau}K_p\omega_n^2\right) & \left(\frac{4}{\tau}K_pT_p\omega_n^2\right) & \left(-\frac{2}{\tau}\right) \end{bmatrix} \begin{bmatrix} x_1 \\ x_2 \\ x_3 \end{bmatrix} + \begin{bmatrix} 0 \\ 1 \\ 0 \end{bmatrix} x_{in}, \quad (3.20)$$

$$x_{out} = \begin{bmatrix} -\omega_n^2 K_p & -\omega_n^2 K_p T_p & 1 \end{bmatrix} \begin{bmatrix} x_1 \\ x_2 \\ x_3 \end{bmatrix}. \quad (3.21)$$

For further theoretical and practical discussions of issues on this scientific topic interested reader can refer to.<sup>1,5,6,8,9,10</sup>

#### 4. Time domain analysis of the human pilot model

One of the most important form of activity of human pilot is reference signal tracking. Many flight tasks (e.g. semi-automated landing, refueling, air-to-air combat, air-to-ground weapon delivery, terrain following, formation flight, aerobatic close formation flight etc.) are in close relationship with this kind of activity. There are some typical input signals to be followed by the pilots, such as step signal, ramp signal, and, much other kind of pure or transformed periodical signals (e.g. saw tooth, square signals etc.). In this paper author chose for the time domain analysis the step input function, the ramp input signal, and finally, the square signal.<sup>1,5,7,11,12,13</sup>

It is well-known from the previous sections that there are several possible mathematical models of human pilot to be used during computer simulation. In this paper we will apply dynamical mathematical model defined by equation (3.3), which is represented in Figure 4. For computer simulation let us use the following parameters of mathematical model of human pilot defined by equation (3.3):

$$K_p = 10; T_p = 1\text{s}; T_1 = 0.4\text{s}; \tau = 0.5\text{s}. \quad (4.1)$$

During computer simulation from possible set of order of approximation there were chosen strongly heuristically the 1st, the 4th, and the 7th orders of approximations. Figure 6 shows step responses of human pilot having approximated mathematical model of time delay. The input signal of human pilot to be followed by him is  $x_{in}(t) = 1(t)$ .<sup>11-13</sup>

From Figure 6 it is obvious that increase of order of approximation result in bigger amplitudes of the output signal. However, in the time delay zone increase of the order of the approximation results in oscillations with higher frequencies having less amplitudes. It means that error of approximation decreases as its order increases.

Figure 7 shows the ramp responses of the human pilot mathematical model. The input signal of the human pilot to be followed by him is  $x_{in}(t) = t$ .

From Figure 7 it is easily can be seen that increase of the order of approximation results in decrease of the error of the approximation: in the time delay zone magnitude of the output signal  $x_{out}(t)$  decreases as order of the approximation is increases while output signal is more and more oscillatory.

Finally, let us analyze the human operator behavior when he is tracking the periodical signal. For this kind of analysis author had chosen the square signal with frequency of  $f=0.3$  Hz, i.e. with period time of  $T=1/f=1/0.3$  s. Results of the computer simulation can be seen in Figure 8.

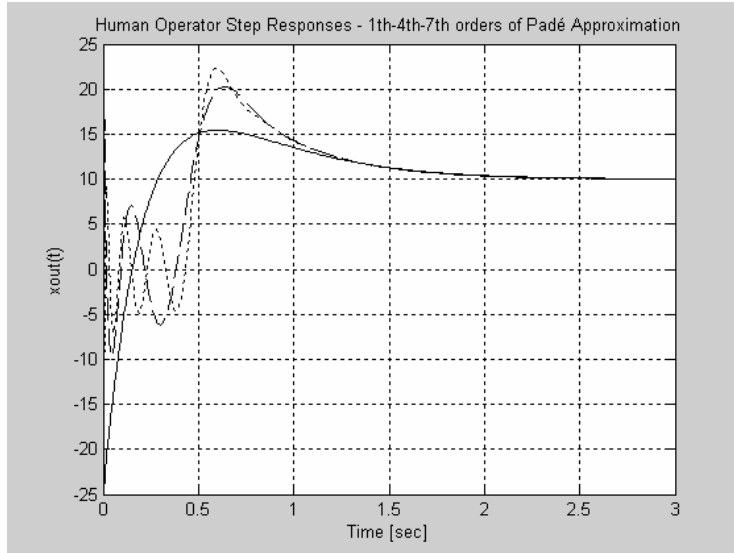


Figure 6. Step responses of the human operator  
'—' 1st '- -' 4th '....' 7th orders of approximation

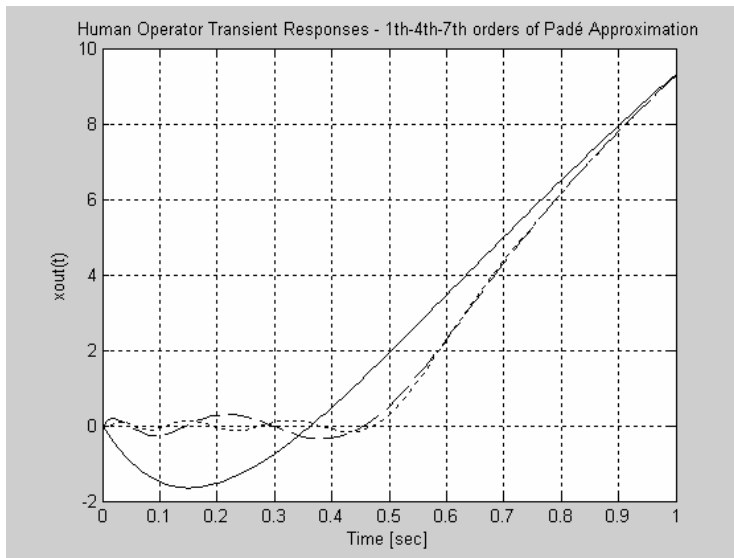


Figure 7. Ramp responses of the human operator  
'—' 1st '- -' 4th '....' 7th orders of approximation

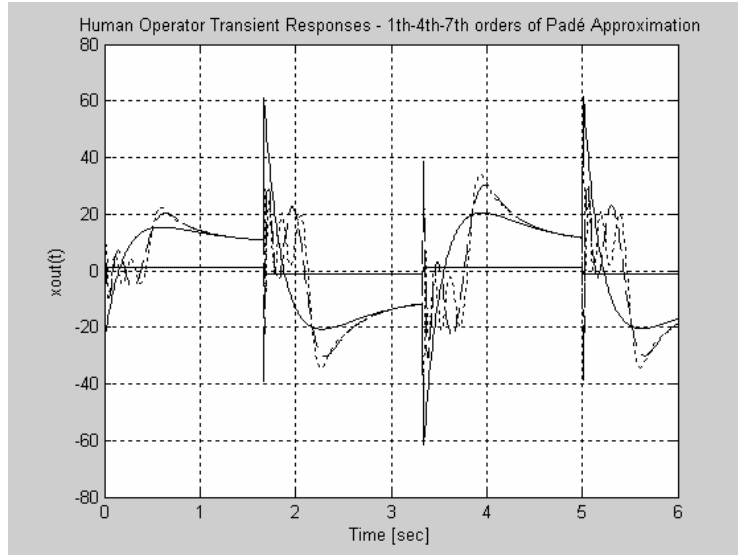


Figure 8. Transient responses of the human operator  
'—' 1st '- -' 4th '....' 7th orders of approximation

From Figure 8 it is easily can be determined that increase of order of approximation results in less amplitudes in output signal. In time delay zone output signal becomes more oscillatory as order of approximations increases.

### 5. Frequency domain analysis of the human pilot

During frequency domain analysis typical input signal of the human pilot is the sinusoidal function changing over some frequency range. Figure 9 shows the response of the human pilot to the harmonic sinusoidal input signal with unity gain.<sup>11,12,13</sup>

From Figure 9 it is obvious that pilot gain for each order of approximation is very close to each other. In the high frequency range the phase angle radically decreases as order of approximation is increases.<sup>11,12,13</sup>

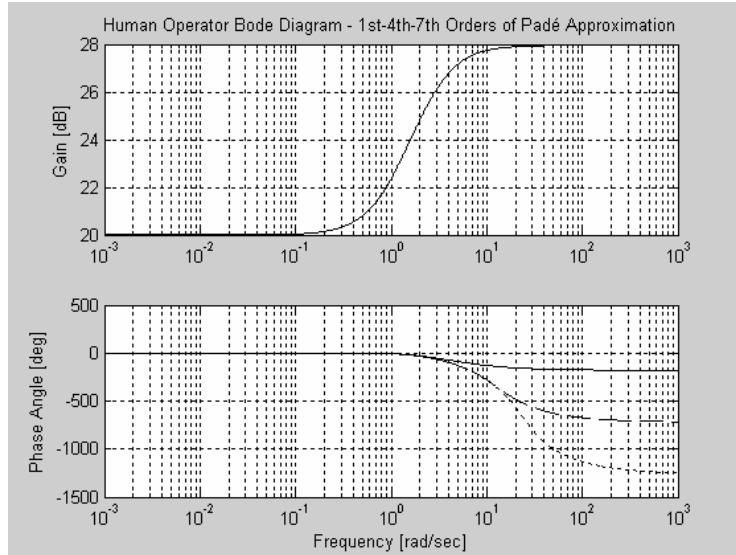


Figure 9. Bode diagrams of the human operator  
 '—', 1<sup>st</sup> '---', 4<sup>th</sup> '....', 7<sup>th</sup> orders of approximation

### 6. Time domain comparison of the human pilot mathematical models

In the practice a question of ‘*what kind of the mathematical model of the pilot activity to use for control system analysis and design?*’ may arise. From theory of automatic flight control systems it is evident that *pilot-in-the-loop* problem can be characterized with multi-loop feature. For instance, during semi-automated landing of the aircraft several flight parameters must be controlled by pilot such as airspeed, vertical speed, height of the flight, distance from runway threshold, glide path angle, angular deflection measured from runway centre line etc. From this follows that increase of number of flight parameters results in decreasing of complexity of the pilot model to be applied during analysis and design of the automatic flight control systems.<sup>1,5,8,9,10</sup>

Let us analyze behavior of human pilot model for several form of its mathematical model while supposing that time delay is approximated by 2nd order Padé-series. During computer simulation mathematical models defined by equations (3.1), (3.2), (3.3) and (3.12) were applied. Results of computer simulation can be seen in Figures 10 to 12. Figure 10 shows step responses of the human pilot behavior, when there was applied to the pilot input the sudden step change in input, say,  $x_{in}(t) = 1(t)$ .

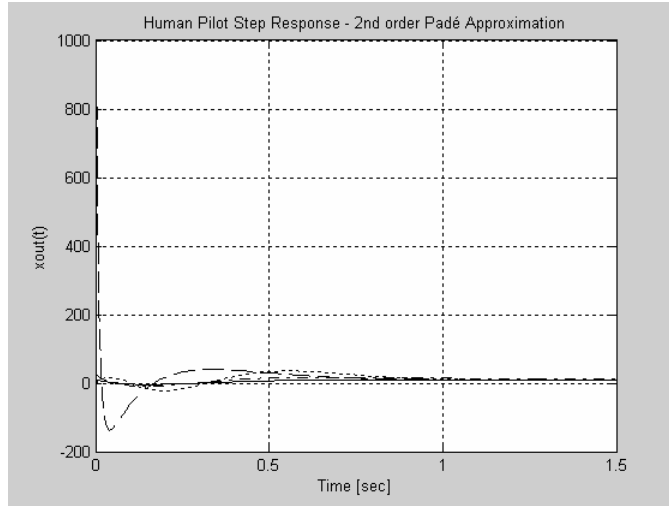


Figure 10. Step responses of the human pilot  
'—' P-TD '---' PD-TD '-.-.' PD-1O-TD '...' PD-2O-TD Models

Figure 11 shows ramp responses of different pilot models having ramp input of  $x_{in}(t) = (t)$ .

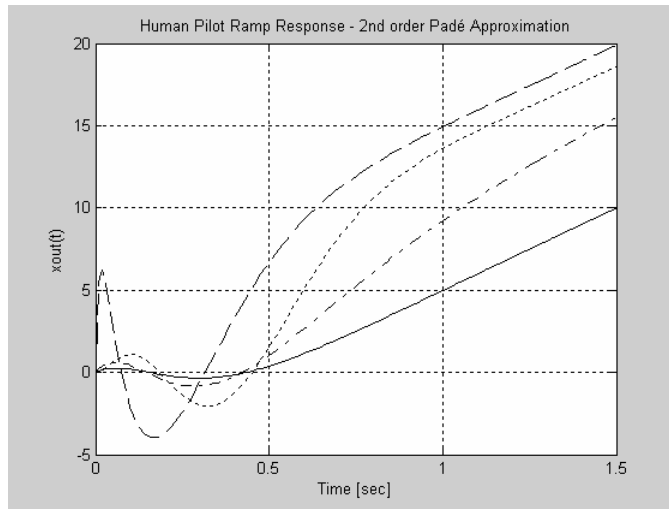


Figure 11. Ramp responses of the human pilot  
'—' P-TD '---' PD-TD '-.-.' PD-1O-TD '...' PD-2O-TD Models

Figure 12 shows transient responses of different human pilot mathematical models induced by applying square periodical signal with unity gain and frequency of 0.3 Hz.

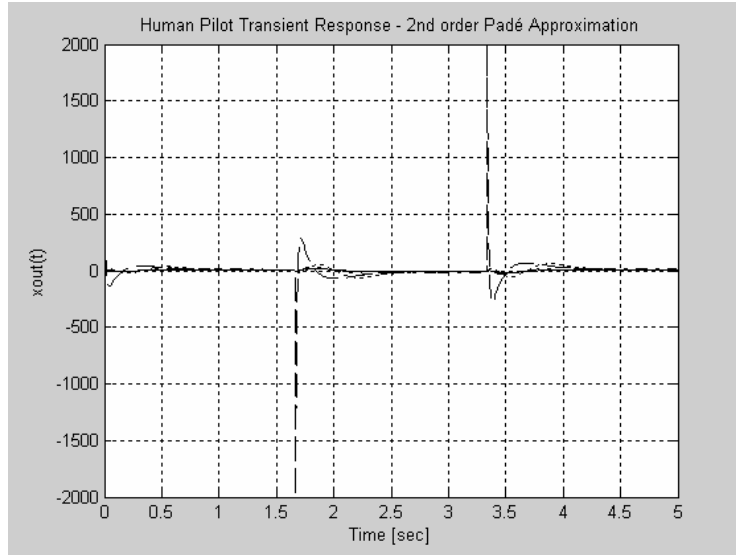


Figure 12. Transient Responses of the Human Pilot  
 ‘—’ P-TD ‘- - -’ PD-TD ‘- . - .’ PD-1O-TD ‘...’ PD-2O-TD Models

Figures 10 to 12 clearly show that if to add the D-term to the proportional (see equation (3.1)) it will result in more oscillatory system (see equation (3.2)) with large amplitudes (dashed line on the figures). Introducing 1st order term to equation (3.2) will result in more damped system reducing oscillatory feature (dash-dot line on Figures 10 to 12). Application of the 2nd order term of equation (3.12), in comparison with system defined by equation (3.3), results in more oscillatory behavior (dotted line on Figures 10 to 12). Using method shown above human pilot model behavior can be compared also for higher orders of the Padé-approximation.

Other interesting question, which arises from here, can be formulated in the following manner: ‘*what is the number of the flight parameters generating need to reduce complexity of the applied mathematical model?*’ The answer to this question cannot be formulated easily. However, the general rule of reducing complexity of the mathematical model while number of flight parameters increase must be applied.<sup>1,5,8,9,10</sup>

### 7. Numerical example of derivation of the minimum order of the Padé approximation

Section 2.1. of this paper dealt with selection of model order to be applied for Padé approximation. There is given a strict mathematical method to derive the order necessary to apply for mathematical modeling of the time delay. Using Figure 1 let us apply other method for model order selection based upon comparison of Nyquist-diagrams of system of  $G(s)$ , which is a transfer function representing the dynamical system with real time delay, and  $\hat{G}(s)$ , which demonstrates approximated mathematical model of the time delay. Present section deals with derivation of the minimum order of the Padé series necessary to apply for given accuracy.

Let the approximation accuracy is defined to be as follows:

$$\delta \leq 0.002. \tag{7.1}$$

For further discussions we will apply P-1O-TD mathematical model of the human pilot. In this particular case transfer function of the pilot can be defined as follows:<sup>1,3,4,5</sup>

$$Y_p(s) = G(s) = \frac{x_{out}(s)}{x_{in}(s)} = \frac{K_p}{1 + sT_1} e^{-s\tau}. \tag{7.2}$$

Frequency response function easily can be derived by substituting  $s = j\omega$  in equation (7.2):<sup>6,7</sup>

$$\begin{aligned} G(s)|_{s=j\omega} &= \frac{x_{out}(j\omega)}{x_{in}(j\omega)} = \frac{K_p}{1 + j\omega T_1} e^{-j\omega\tau} = \\ &= \frac{K_p(1 - j\omega T_1)}{1 + (\omega T_1)^2} e^{-j\omega\tau} = P_{TD}(\omega) + jQ_{TD}(\omega) \end{aligned} \tag{7.3}$$

In equation (7.3) introduce following terms:

$$P_{TD}(\omega) = \text{real} \left( \frac{K_p(1 - j\omega T_1)}{1 + (\omega T_1)^2} e^{-j\omega\tau} \right), \tag{7.4}$$

which is real part of frequency response function of  $G(j\omega)$ , and,

$$Q_{TD}(\omega) = \text{imag} \left( \frac{K_p(1 - j\omega T_1)}{1 + (\omega T_1)^2} e^{-j\omega\tau} \right). \tag{7.5}$$

which is imaginary part of  $G(j\omega)$ .



Approximated mathematical model of human pilot can be given as:

$$\hat{G}(s) = \frac{x_{out}(s)}{x_{in}(s)} \cong \frac{K_p}{1 + sT_1} P_d(s). \quad (7.6)$$

Frequency response function of the approximated system of  $\hat{G}(s)$  can be derived by substituting  $s = j\omega$ .<sup>6,7</sup>

$$\begin{aligned} \hat{G}(j\omega) &= \frac{x_{out}(j\omega)}{x_{in}(j\omega)} \cong \frac{K_p}{1 + j\omega T_1} P_d(j\omega) = \\ &= \frac{K_p(1 - j\omega T_1)}{1 + (\omega T_1)^2} \frac{1 - \frac{1}{2}(j\omega\tau) + \frac{1}{12}(j\omega\tau)^2 + \dots}{1 + \frac{1}{2}(j\omega\tau) + \frac{1}{12}(j\omega\tau)^2 + \dots}. \end{aligned} \quad (7.7)$$

Transforming frequency response function  $\hat{G}(j\omega)$  to its complex algebraic form yields to following equation:

$$\begin{aligned} \hat{G}(j\omega) &\cong \frac{K_p(1 - j\omega T_1)}{1 + (\omega T_1)^2} \frac{1 - \frac{1}{2}(j\omega\tau) + \frac{1}{12}(j\omega\tau)^2 + \dots}{1 + \frac{1}{2}(j\omega\tau) + \frac{1}{12}(j\omega\tau)^2 + \dots} = \\ &= P_{APPR.}(\omega) + jQ_{APPR.}(\omega) \end{aligned} \quad (7.8)$$

Real part of  $\hat{G}(j\omega)$  can be written as:

$$P_{APPR.}(j\omega) \cong \text{real} \left( \frac{K_p(1 - j\omega T_1)}{1 + (\omega T_1)^2} \frac{1 - \frac{1}{2}(j\omega\tau) + \frac{1}{12}(j\omega\tau)^2 + \dots}{1 + \frac{1}{2}(j\omega\tau) + \frac{1}{12}(j\omega\tau)^2 + \dots} \right) \quad (7.9)$$

and, imaginary part of  $\hat{G}(j\omega)$  is as follows:

$$Q_{APPR.}(j\omega) \cong \text{imag} \left( \frac{K_p(1 - j\omega T_1)}{1 + (\omega T_1)^2} \frac{1 - \frac{1}{2}(j\omega\tau) + \frac{1}{12}(j\omega\tau)^2 + \dots}{1 + \frac{1}{2}(j\omega\tau) + \frac{1}{12}(j\omega\tau)^2 + \dots} \right). \quad (7.10)$$

Order of the Padé approximation, of course starting with the first, must be increased until following inequalities take place:

$$P_{TD}(\omega) - P_{APPR.}(\omega) \leq \delta, \tag{7.11}$$

and

$$Q_{TD}(\omega) - Q_{APPR.}(\omega) \leq \delta. \tag{7.12}$$

The order of Padé approximation, which results in inequalities (7.11)–(7.12) is minimum order to be used for analysis and design purposes.

To demonstrate a numerical example let us have following pilot model to be approximated:

$$Y_p(s) = G(s) = \frac{x_{out}(s)}{x_{in}(s)} = \frac{K_p}{1 + sT_1} e^{-s\tau} = \frac{10}{1 + 0,4s} e^{-0,5s} \tag{7.13}$$

This mathematical model was approximated by linear model of  $\hat{G}(j\omega)$  defined by equation (7.6). Nyquist plots for both systems derived by  $G(j\omega)$  and  $\hat{G}(j\omega)$  were found and plot in Figure 13.

For Nyquist diagrams frequency range was chosen to be  $\omega=(0-10)$ rad/s, which represents range of the possible input signals of the human pilot. In Table 1. solid lines show Nyquist plots of  $G(j\omega)$ , which is model of human pilot having time delay of  $\tau$ . In Figure 13 the dotted lines show Nyquist plots of  $\hat{G}(j\omega)$ , which is approximated mathematical model of the human pilot. From Table 1. it is evident that any increase of order of the Padé approximation results in decrease of the error of the approximation. Approximation errors were calculated and put in Figure 14.

Table 1. Approximation errors

Order of Padé approximation	Differences ( $\Delta P, \Delta Q$ )	
	$\Delta P = P_{TD}(\omega) - P_{APPR.}(\omega)$	$\Delta Q = Q_{TD}(\omega) - Q_{APPR.}(\omega)$
$n = 1$	4.7642	3.3276
$n = 2$	1.5617	0.4369
$n = 3$	0.2317	0.0297
$n = 4$	0.0204	0.0012
$n = 5$	0.0012	$3.1697 \cdot 10^{-5}$
$n = 6$	$4.5377 \cdot 10^{-5}$	$5.8809 \cdot 10^{-7}$

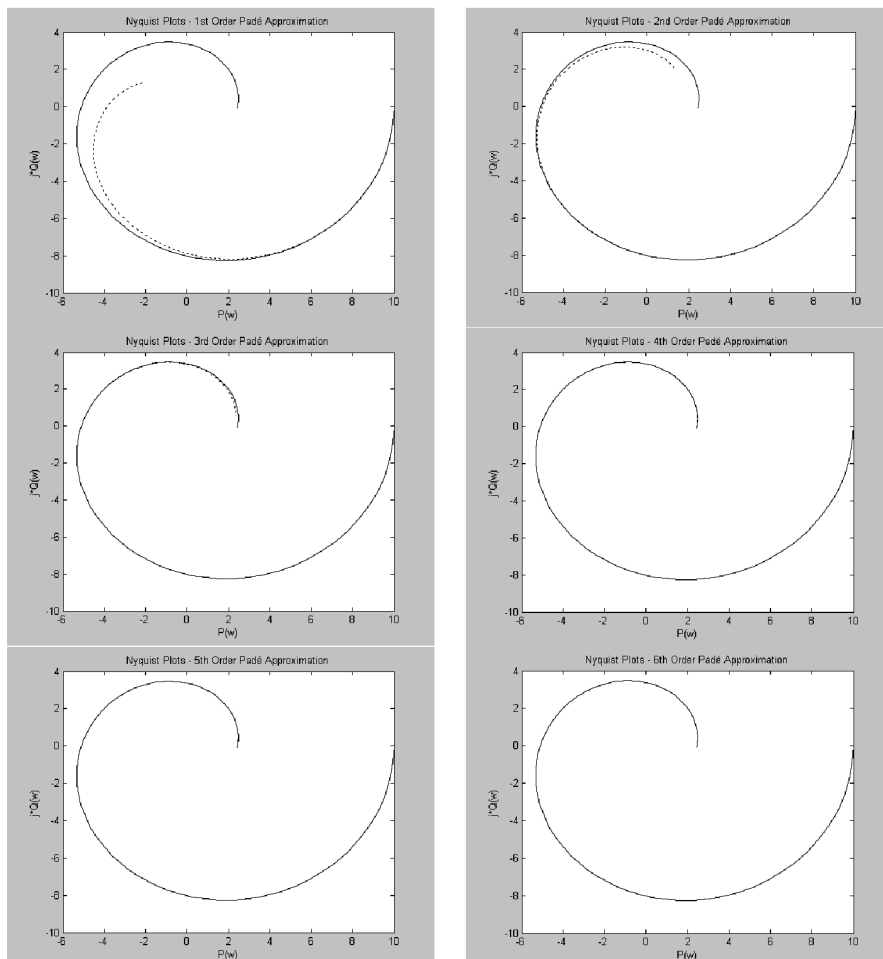


Figure 13. Nyquist plots of systems of  $G(j\omega)$  and  $\hat{G}(j\omega)$ .  
 Solid line: Nyquist Plot of  $G(j\omega)$ , dotted line: Nyquist Plot of  $\hat{G}(j\omega)$ .

From Table 1, it is clear that for  $n=4$  tolerances defined by equations (7.11)–(7.12) are very close to that of defined by equation (7.1). Next approximation applied for  $n=5$  results in very small deviations, which show that for the given time delay of  $\tau=0.5$  s the minimum order of the Padé approximation to have mismatch of  $\approx 0.02$ , of the original system of  $G(j\omega)$ , and the approximated system of  $\hat{G}(j\omega)$ , defined by equations (7.3),

and (7.7), respectively, is  $n=5$ . For  $n=5$  Padé series can be determined using equation (2.5) to be:

$$e^{-0,5s} \cong P_d(s) = \frac{1 - \frac{1}{2!} \tau s + \frac{2!}{4!} (\tau s)^2 - \frac{3!}{6!} (\tau s)^3 + \frac{4!}{8!} (\tau s)^4 - \frac{5!}{10!} (\tau s)^5}{1 + \frac{1}{2!} \tau s + \frac{2!}{4!} (\tau s)^2 + \frac{3!}{6!} (\tau s)^3 + \frac{4!}{8!} (\tau s)^4 + \frac{5!}{10!} (\tau s)^5} \quad (7.14)$$

Figures 14 and 15 show errors in the real and in the imaginary parts of the frequency response functions derived by equations (7.11)–(7.12), respectively.

Figure 14 shows deviations of the real parts of the frequency response functions of two dynamical systems of  $G(j\omega)$  and  $\hat{G}(j\omega)$ , in increasing order of the Padé approximation. It is easily can be stated that deviations between the time delay system  $G(j\omega)$ , and the approximated system  $\hat{G}(j\omega)$  decreases as order of the Padé approximation is increases.

Note that for the given order of the approximation the approximation error increases as input signal frequency approaches to its maximum bound. In low frequency domain the error is sufficiently less that of belonging to high input signal frequency.

Figure 15 shows deviations of the imaginary parts of the frequency response functions of two dynamical systems of  $G(j\omega)$  and  $\hat{G}(j\omega)$ . It is easily can be seen that any increase of the order of the approximation results in decreasing deviation of the time delay system of  $G(j\omega)$ , and of the approximated system of  $\hat{G}(j\omega)$ . For the given order of the Padé approximation deviation increases as frequency increases and goes to its maximum value of 10 rad/s.

From the diagrams of Figure 15 it is evident that order of the Padé approximation of  $n=5$  satisfies requirement defined preliminary by equation (7.1). In other words, time delay of equation (7.13) can be approximated by equation (7.14) within the tolerance of  $d \leq 0.02$ .

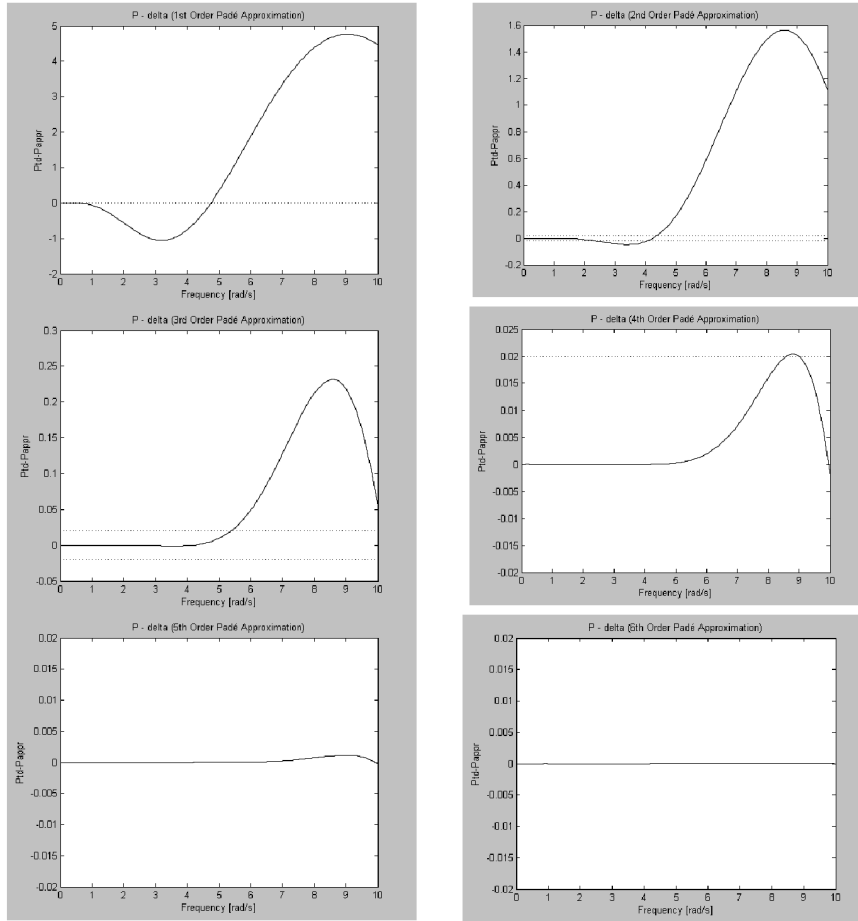


Figure 14.  $P_{TD}(\omega)-P_{APPR}(\omega)$  vs. frequency.  
 Solid line:  $P_{TD}(\omega)-P_{APPR}(\omega)$ , dotted line:  $\delta=0.02$

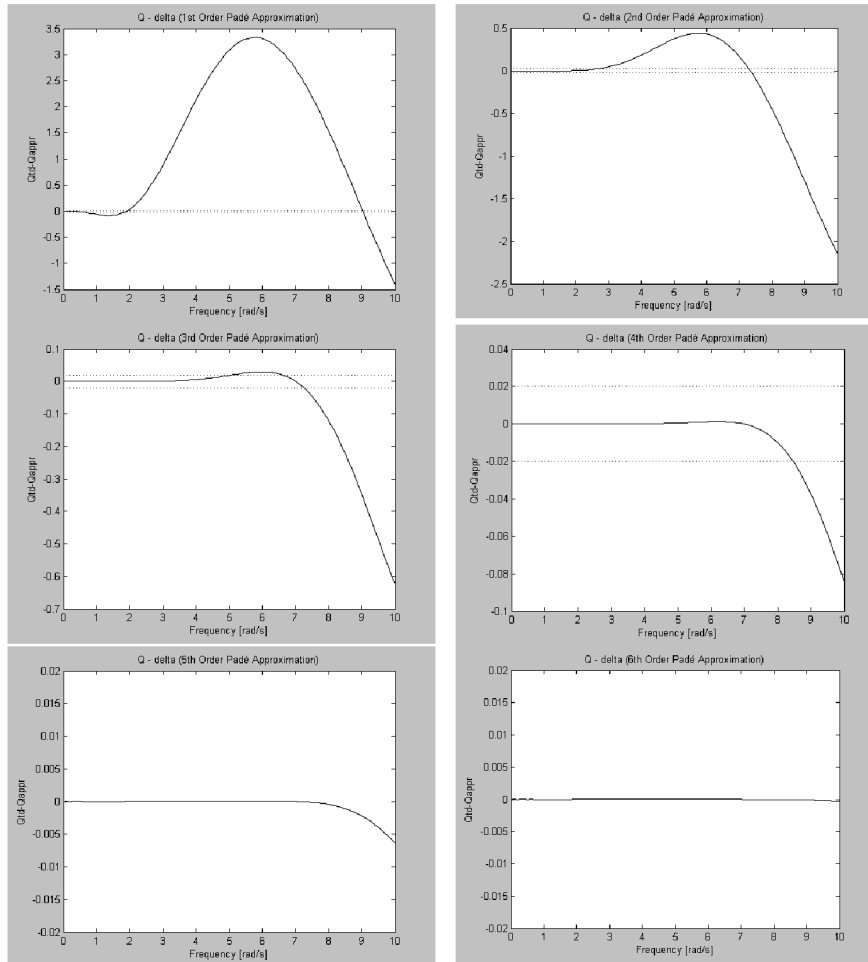


Figure 15.  $Q_{TD}(\omega) - Q_{APPR}(\omega)$  vs. frequency.  
 Solid line:  $Q_{TD}(\omega) - Q_{APPR}(\omega)$ , dotted line:  $\delta = 0.02$

## 8. Conclusions

Human operator still one of the most ‘important part’ of the automatic control systems. They may monitor, or actively actuate in the control systems. Since he acts as ‘simple term’ of the closed loop control system it is necessary to model his activity, and, take

this into consideration. Modeling human pilots is important from many aspects of aircraft maintenance both in the air and on the ground. Human pilot mathematical model depends upon complexity of the system in which he acts, upon the level of his training, upon his physical and psychical conditions.

In most cases as scalar tolerance  $\delta$  decreases,  $\omega_x$  increases (see equation (2.9)) and this forces order of approximation  $n$  to increase. Obviously, for very large values of  $n$  the relative magnitude of  $c_0/c_n$  of the coefficients of transfer function of  $P_d(s)$  becomes very large. In this case numerical difficulties may arise in computer aided analysis and simulation process. On the other hand, as time delay  $\tau$  increases, order of approximation  $n$  also should be increased to keep the approximation error  $\delta$  limited regarding pre-defined qualitative requirements.

Regarding *pade.m* built-in function of MATLAB computer program it is easily can be derived that in case of  $\tau=0.5$  s and  $n \leq 67$  program calculates well. At higher orders of approximation, say, for  $n > 68$ , program starts to fail and in the time delay zone oscillations may appear with increased amplitudes.

In Section 2.1. author proposed method for selection of order of Padé-approximation, which is easily can be applied for Padé series minimum order selection. In Section 7 Nyquist-method was applied for deriving minimum order of the Padé approximation. A numerical example was explained and for the given inaccuracy the minimum order of the Padé approximation was found to be  $n=5$ . This simple heuristic method is widely applied in automatic control theory. Mathematical model given by equation (7.14) approximating original time delay of  $\tau=0.5$  s is quiet complicated, but gives accurate approximation of the time delay. This It can be used with no difficulties for preliminary design of automatic control systems and for system analysis.

## References

1. MCRUER, D. T., KRENDEL, E. S., *Mathematical Models for Human Pilot Behavior*, NATO Advisory Group for Aerospace Research and Development, AGARDograph AG 188, 1974.
2. KORN, G. A., KORN, T. M., *Mathematical Handbook for Scientists and Engineers*, Technical Publishing Co., Budapest, 1975 (in Hungarian).
3. ASLANYAN, A. E. *Aircraft Automatic Flight Control Systems of the Aircraft*, Part I, Air Force Institute of Kiev, Kiev, 1984 (in Russian).
4. KRASOVSKY, A. A., VAVILOV, JU. A., SUTCHKOV, A. I., *Automatic Flight Control Systems*, Air Force Academy of Joukowsky, Moscow, 1986 (in Russian).
5. MCLEAN, D., *Automatic Flight Control Systems*, Prentice-Hall International, New York-London-Toronto-Sydney-Tokyo-Singapore, 1990.
6. DORF, R. C., BISHOP, R. H., *Modern Control Systems*, Prentice Hall International, Upper Saddle River, New Jersey, 2001.

R. SZABOLCSI: Modeling of the human pilot time delay using Padé series

7. LANTOS, B. *Control Systems Theory and Design*, Part I-II, Academic Publishing Co., Budapest, 2001 (in Hungarian).
8. SZABOLCSI, R. *Conventional and Modern Mathematical Models Applied to model Pilot Behavior in the Flight Control Systems*, Proceedings of the Scientific Conference 'New Century, New Technology – Gripen in the Hungarian Air Force', CD-ROM, 21 April 2006, Szolnok, Hungary (in Hungarian).
9. SZABOLCSI, R., *Derivation of the Pilot's Critical Parameters Affecting Flight Safety*, Scientific Bulletins, Vol. 2006/3., pp (13–24), University of Debrecen, Debrecen, 2006 (in Hungarian).
10. SZABOLCSI, R. *Complex Analysis of the Pilot's Critical Parameters in the Lateral Motion Flight Control Systems*, Bulletins in Aeronautical Sciences, Vol. 2006/1, pp (97–117), Szolnok, 2006 (in Hungarian).

### Software manuals

11. *MATLAB*<sup>®</sup> 5.2 – *The Language of Technical Computing*, User's Guide, The MathWorks, Inc., 1997.
12. *MATLAB*<sup>®</sup> 6.5 — *The Language of Technical Computing*, User's Guide, The MathWorks, Inc., 2002.
13. *Control System Toolbox 5.1 for Use With MATLAB*<sup>®</sup> (Release 12.1), User's Guide, The MathWorks, Inc., 2001.